Centrifuge Test for Seismic Response of SDOF Structures with Shallow Foundation

D.K. Kim & H.G. Park
Seoul National University, Korea

D.S. Kim & Y.W. Choo
Korea Advanced Institute of Science and Technology, Korea

S.H. Lee
Korea Institute of Nuclear Safety, Korea

SUMMARY
In order to evaluate the seismic force to structures amplified by soft soil deposits, centrifugal tests were performed. The test specimen was composed of a Single-Degree-of-Freedom structure model, a shallow foundation and sub-soil deposits in a centrifuge container. In this test, being accompanied by the centrifugal acceleration, horizontal earthquake accelerations were applied to the container by a shaking table. The test parameters were the dynamic periods of the SDOF structure models, centrifugal acceleration level, types of input earthquake acceleration, and peak acceleration level of the earthquakes. The test results showed that the mass and stiffness of the structure affected the nonlinear behaviour of the sub-soil beneath the shallow foundation as well as its own response. Unlike expectation, the lateral forces and displacements of the structure models were not significantly amplified by the soft sub-soils. Thus, the lateral forces resulting from the combined effect of structure and sub-soil in the test model were less than the lateral forces calculated from the conventional fixed base model neglecting soil-structure interaction. On the other hand, the overturning moment and the resulting rocking displacement (or rotation) were significantly amplified by the soil-structure interaction. The rocking displacements increased the damping effect of the sub-soil by increasing the nonlinear soil strain. For this reason, the rocking effect decreased the lateral displacements of the structures.

Keywords: centrifuge test, soil-structure interaction, shallow foundation, rocking effect

1. INTRODUCTION

It is important to expect exactly the seismic load of a building, which is amplified by the soft sub-soil deposits, to design the building or to evaluate the seismic demand of the building. Therefore, a number of numerical analysis studies (Hwang et al. (1997), Kim et al. (2006), MAE center (1999)) have been performed to estimate the seismic lateral force of structures under earthquake motion. The numerical analyses have shown the dynamic responses of the structures amplified by the resonance between the structures and the site period. Based on the analytical results, many design response spectra (ICC (2009), European Committee for Standardization (2003), Tena-Colunga et al. (2009)) have been proposed to describe accurately the seismic load according to the site condition.

On the other hand, the 1997 Federal Emergency Management Agency NEHRP Guidelines for the seismic retrofit of buildings and the associated Applied Technology Council document (ATC 40) discuss alternative design methods associated with the response of shear walls when subjected to lateral earthquake induced rocking (NEHRP (1997), Comartin et al. (2000)). The rocking effect acts as an energy dissipation mechanism, but the mechanism may result in permanent deformations (settlement, rotation or sliding) (Gajan et al. (2005)).

To verify the seismic load and the design method for the structure with the shallow foundation, various centrifugal tests have been performed. Gajan et al. (2005) performed centrifugal tests including 40 models of shear wall footings to study the nonlinear load-deformation characteristics during cyclic and earthquake loading. Based on the experimental results, Gajan and Kutter (2008) observed capacity, settlement and energy dissipation of shallow footings subjected to the rocking. As a numerical model, a contact interface model for the shallow foundation was proposed by Gajan and Kutter (2009). Curras et al. (2001) obtained experimental data on the seismic response of a pile-group-supported structure though dynamic centrifuge model tests. And the experimental results provide support for the use of dynamic beam on a nonlinear Winkler foundation (BNWF) analysis model.

In this study, centrifugal tests were performed to evaluate the dynamic responses of structures with a shallow foundation. A primary testing variable was the period of the super-structure. Seven structures with varying the period were used to investigate the dynamic interaction between the structure and the site period. To realize the actual gravitational stresses of a prototype structure and sub-soil, amplified centrifugal accelerations were given to the small scale model of structure and sub-soil deposit. Accompanied by the centrifugal acceleration, horizontal earthquake accelerations were given to the subsoil container by a shaking table. By performing centrifugal tests, the lateral displacements and rocking angle of the structure and foundation were investigated. On the basis of the results, the seismic force amplified by the soft soil deposits was evaluated, and it was compared with the lateral force calculated by a conventional design method using fixed base model with free field surface acceleration. The test parameters were the dynamic periods of the SDOF structure models, centrifugal acceleration level, types of horizontal earthquake accelerations, and peak acceleration level of the earthquakes.

2. TEST PROGRAM

2.1. Test Specimen

The test specimen was composed of a Single-Degree-of-Freedom (SDOF) structure model, a shallow foundation and sub-soil deposits in a centrifuge container. The SDOF structure was composed of a lumped mass on the top and two thin plates representing the lateral stiffness of the structure. The SDOF structure was made of steel. By using the two separated plates, the structure model was designed to show the shear-deformation mode. Three types of the stiffness of the structure were used. And by adding a mass to the structure, the period of the structure was lengthen without change of the stiffness. Table 2.1 shows the properties of the small-scale SDOF structure models in 1g and the dynamic properties of the prototype structures in 20 and 40 centrifugal acceleration (gc).

Natural frequency of the small-scale SDOF structure model was measured by impact hammer testing and FFT analysis. Effective mass including the lumped mass on the top and a portion of the plates and stiffness of the plates considering the welding connection were calculated from the natural frequency. Damping ratio of the small-scale SDOF structure was calculated from decline of the response by the impact hammer testing (Chopra (2007)). Foundation contact pressure is a pressure at the bottom of the foundation resulting from the total weight of the SDOF structure and the foundation. As the centrifugal acceleration increased, the stresses of the small-scale structure and the foundation contract pressure increased. Thus, the stresses of the prototype were simulated.

Table 2.1. Properties of SDOF structures

structures	SDOF1	SDOF2	SDOF3	SDOF4	SDOF5	SDOF6	SDOF7
dimension (mm)	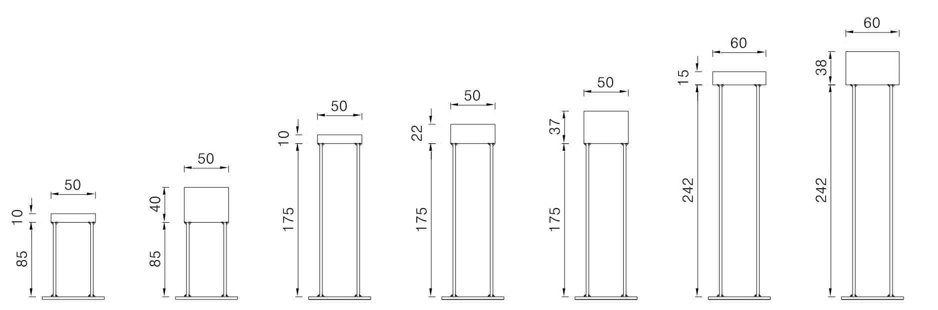						

Table 2.1. Properties of SDOF structures (Cont.)

structures	SDOF1	SDOF2	SDOF3	SDOF4	SDOF5	SDOF6	SDOF7
effective mass (kg)	0.229	0.866	0.270	0.506	0.800	0.663	1.131
stiffness (kN/m)	461.6	461.6	60.45	60.45	60.45	22.86	22.86
natural frequency (Hz)	226	116	76	56	44	30	20
natural period (sec)	0.0045	0.0085	0.0132	0.0179	0.0227	0.0333	0.0500
T_n @20gc[1)] (sec)	0.09	0.17	0.26	0.36	0.45	0.66	1.00
T_n @40gc[1)] (sec)	0.18	0.34	0.52	0.72	0.90	1.32	2.00
damping ratio (ξ)	0.009	0.007	0.022	0.015	0.014	0.017	0.021
foundation contact pressure @20gc (kPa)	26.2	49.7	32.8	42.2	54.0	45.7	71.7
foundation contact pressure @40gc (kPa)	52.3	99.4	65.6	84.4	108.0	91.4	143.4
FS_V[2)]	14.0	7.4	11.2	8.7	6.8	8.0	5.1

[1)]gc = centrifugal acceleration (g)
[2)] FS_V = factor of safety for vertical load

The shallow foundation was made of aluminum and composed of a box. The external and internal dimensions of the shallow foundation were 70mm x 70mm x 30mm, and 50mm x 50mm x 20mm (length x width x depth). The weight of the foundation was similar to that of the soil with the same external volume. The exterior panel of the soil container is composed of shear beams so that the horizontal movement of the soil is allowed to reduce the reflection of the waves at the boundary of the container. A horizontal shaking table is attached to the container, to simulate earthquake motions. The external and internal dimensions of the soil container were 0.6m x 0.6m x 0.6m, and 0.49m x 0.49m x 0.6m (length x width x depth) (Figure 1). Under 40g of spin acceleration, the internal size of the soil in the container became equivalent to a prototype soil with a volume of 19.6m x 19.6m x 24m.

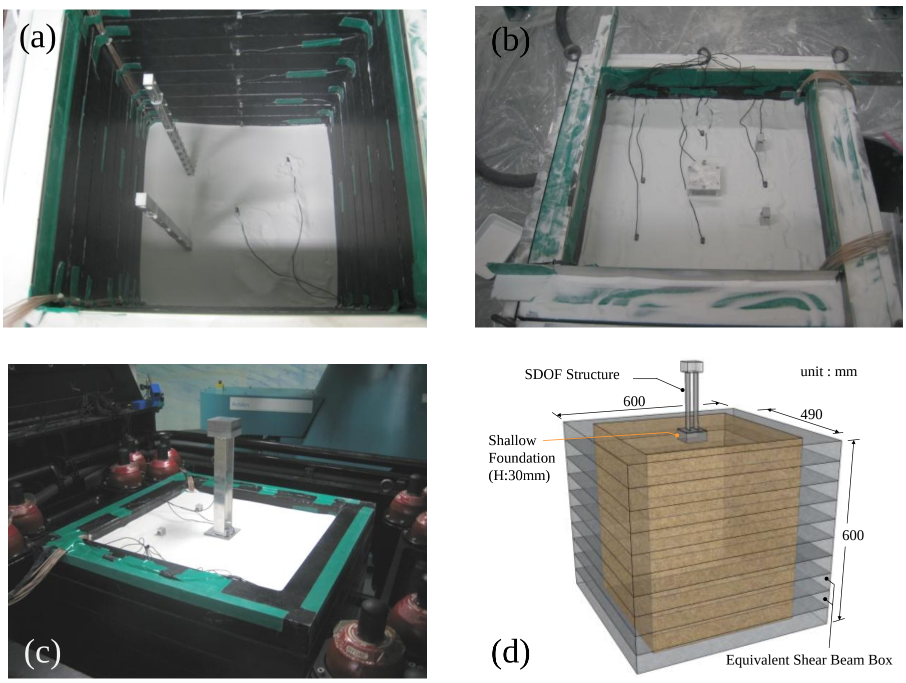

Figure 1. Construction of test specimen in equivalent shear beam container

2.2. Soil Properties

The soil in the container was placed using a sand-rainer to simulate the target relative density, 85%. The shear-wave velocities of the soil strata were measured by the cross-hole seismic method using bender element array under the centrifugal acceleration. Figure 2 shows the shear-wave velocity profiles of the soil. The shear-wave velocity profiles from the cross-hole seismic method were very similar to those of the resonant column tests. The average shear wave velocities were 194m/s @ 20gc (centrifugal acceleration = 20g) and 234 m/s @ 40gc. By the site classification of IBC 2009, the site class is S_D, which is a very soft soil. However, the site period was estimated to be 0.25 sec. and 0.41 sec. for the two soils because of the shallow soil thickness. Table 2.2 summarized the soil properties.

Table 2.2. Soil Properties

Soil thickness (small model)	Mass density	Relative density	Centrifugal acceleration	Soil thickness (prototype)	Average shear wave velocity	Average shear modulus	Site period (calculation)
60 cm	1.55 ton/m^3	85 %	20g	12 m	194 m/s	58.3 MPa	0.25 s
			40g	24 m	234 m/s	84.8 MPa	0.41 s

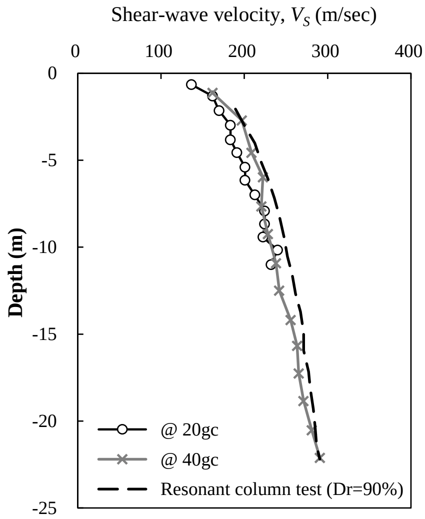

Figure 2. Shear-wave velocity profile

The ultimate moment capacity of the rocking foundation can be determined by Eqn. 2.1. As the foundation rocks, a contact area between the foundation and the rounded soil moves from one site of the foundation to the other in Figure 3.

$$M_{ult} = \frac{V \cdot L_f}{2} \cdot \left(1 - \frac{L_c}{L_f}\right) \tag{2.1}$$

where V is the vertical load on the foundation; L_f is the foundation length in shaking direction; L_c is critical contact length required to support the vertical load. The ratio L_f/L_c is approximately equal to the traditional factor of safety FS_V against bearing failure (Kutter et al. (2010)). Therefore ultimate bearing capacity of square foundation was calculated by Terzaghi's equation (DAS (2007)). Because the soil was silica-sand, cohesion of soil c' was zero. From triaxial test, friction angle φ was 30 degree. The factor of safety FS_V of each SDOF structure was calculated in Table 1.

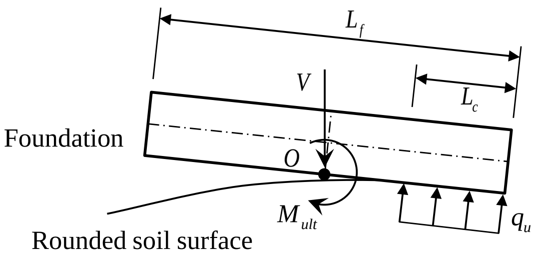

Figure 3. Geometry and contact of the foundation with deformed soil surface

2.3. Input Accelerations

To investigate actual responses of the structure with the shallow foundation, two real earthquake accelerations were applied to the base of the ESB box. 1994 Northridge earthquake and 1995 Kobe earthquake were used. Dominant frequencies of the Northridge earthquake range from 0.6 Hz to 2.9 Hz, and the Northridge earthquake represents long period waves. Dominant frequencies of the Kobe earthquake range from 1.35 Hz to 2.8 Hz, and the Kobe earthquake represents short period waves. From 0.05g to 0.4g, the peak accelerations of the base excitation gradually increased.

3. TEST RESULT

Because displacements of the small-scale structure and the foundation were very small in the ESB container, displacement meters were not available. Thus, to investigate the dynamic responses of the structure model and foundation, accelerations of the structure and the foundations were measured. The recorded accelerations and time step in centrifugal acceleration '*N*'g were scaled by the scaling laws (Schofield 1980) to represent the accelerations of the prototype structures in 1g. The scaled accelerations were converted to displacements by using a high-pass filter and the double integration method. When the high-pass filter was not used, the displacements from the measured accelerations diverged. And it is ambiguous to determine cut-off frequency of the high-pass filter. Because the dynamic responses of the structure depend on the period of the structure, it is not reasonable to use a single cut-off frequency for the seven SDOF structures. In this study the cut-off frequency was determined by Eqn. 3.1, which includes the translation of the structure and the foundation and the rocking of the foundation. And Figure 4 shows the relations between the displacements of the structure and the foundation.

$$m_s\ddot{u}_t + c_s(\dot{u}_t - \dot{u}_f - h\cdot\dot{u}_\theta) + k_s(u_t - u_f - h\cdot u_\theta) = 0 \tag{3.1}$$

$$u_\theta = \left(u_{v1} - u_{v2}\right)/L_f \tag{3.2}$$

where u_t = total displacement of the structure, u_{v1} and u_{v2} = vertical displacements of the foundation, u_f = horizontal displacement of the foundation. From the vertical displacements, the rocking angle u_θ of the foundation was calculated as Eqn. 3.2.

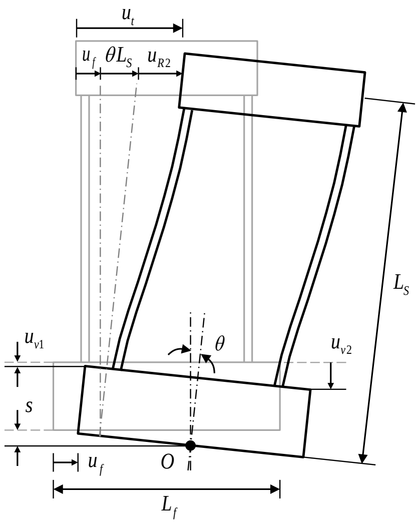

Figure 4. Displacements of SDOF structure

$$\ddot{u}_t = \frac{-c_s(\dot{u}_t - \dot{u}_f - h \cdot \dot{u}_\theta) - k_s(u_t - u_f - h \cdot u_\theta)}{m_s} \tag{3.3}$$

Eqn. 3.1 can be expressed as Eqn. 3.3. The left term is the measured acceleration and the right term is acceleration quantity calculated from the velocities and displacements, which are integrated from the filtered accelerations. On the basis of Eqn. 3.3, the cut-off frequency, which made the coincidence between the left term and the right, was determined. Figure 5 shows that the right term in Eqn. 3.3 agree with the measured acceleration on magnitude and shape of the acceleration.

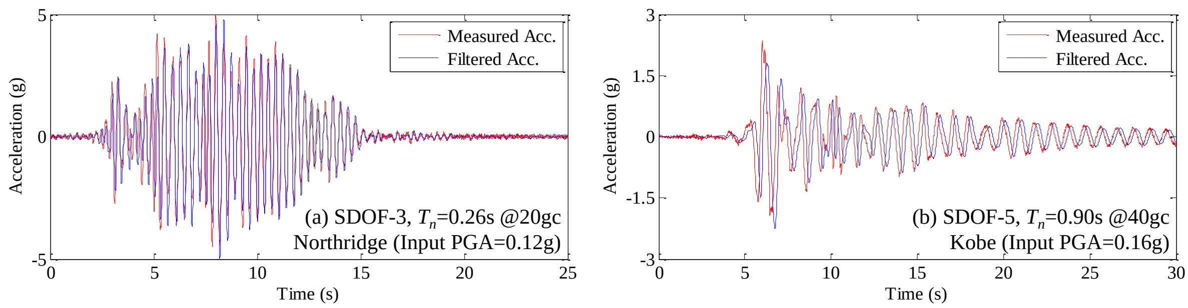

Figure 5. Coincidence of measured and filtered accelerations

The net lateral displacements of the structure model including and excluding the rocking effect can be calculated as follows. The net lateral displacements were compared with predicted displacements u_{fixed} by using the fixed base model and free field surface accelerations.

$$u_{R1} = u_t - u_f \tag{3.4}$$

$$u_{R2} = u_{R1} - \theta L_s \tag{3.5}$$

Figure 6 shows the dynamic responses of seven structure models. The period of the prototype soil deposit was 0.25 sec. The input earthquake was the Northridge earthquake and the peak acceleration was 0.22g. In case of the structure model with T_n=0.09s @ 20g as shown in Figure 6(a), because of the large stiffness of the structure, the net displacement of the structure model was very small. Figures 6(b) ~ (e) show the responses of the structure models with periods of 0.17s ~ 0.45s @ 20g. In the figure, u_{R1} was much greater than u_{R2}, which indicates that the rocking effect was significant. However, the displacements of the structure model u_{R2} (or u_{R1}) was significantly smaller than the displacement u_{fixed} predicted by using the fixed base model and free-field ground motion. This result showed that the rocking effect or the soil-structure interaction significantly decreased the inertia force of the structure model.

Figures 6(f) and (g) show the responses of the structures with periods of 0.66s and 1.00s @ 20g. The periods of the structure models were significantly different from the period of the soil deposit, 0.25sec. As shown in the figures, in this case, the rocking effect was very small. The response of the structure model was close to that of the fixed base model.

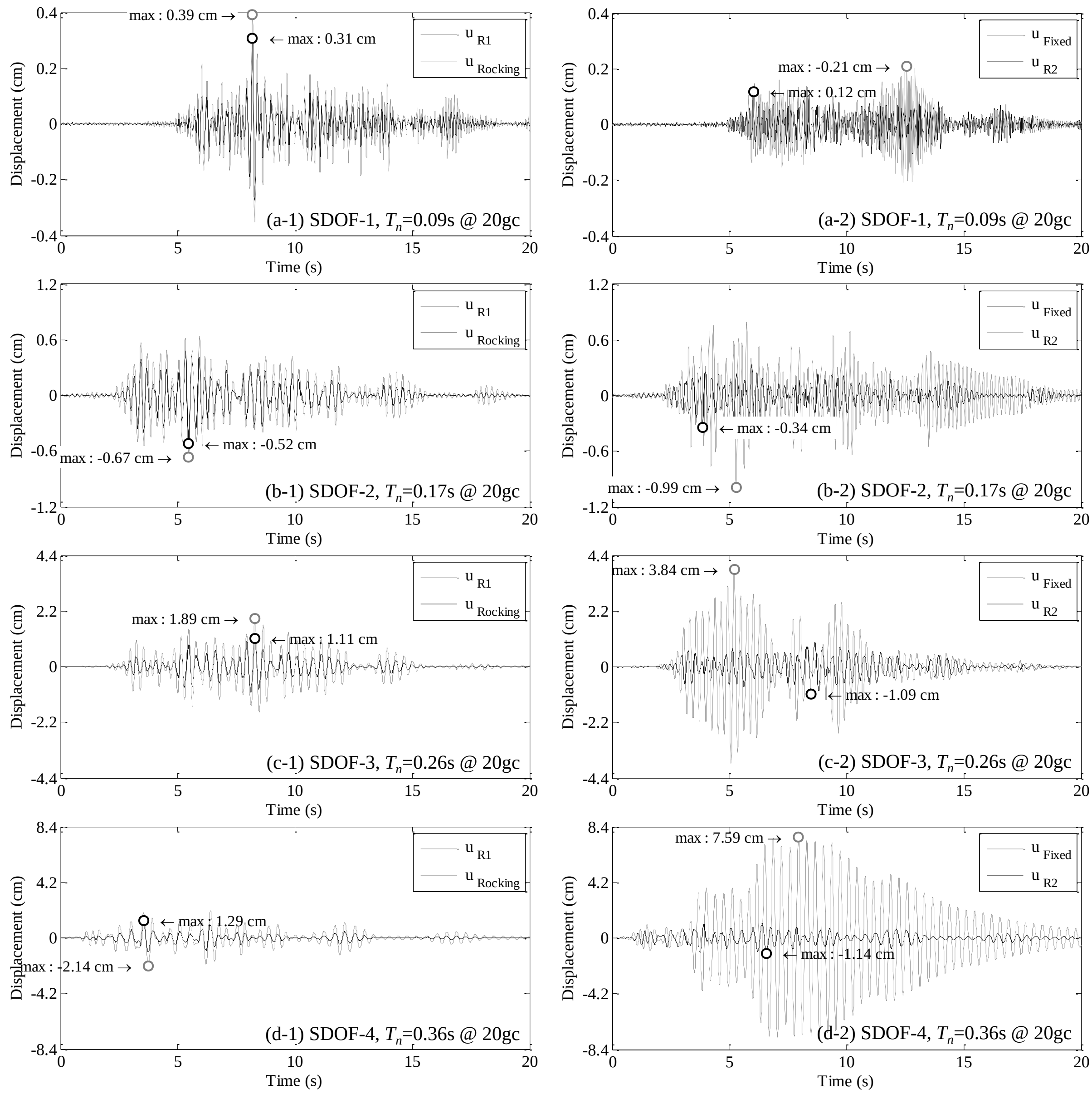

Figure 6. Displacement time history responses of structure models (Northridge, Input PGA=0.22~0.24g)

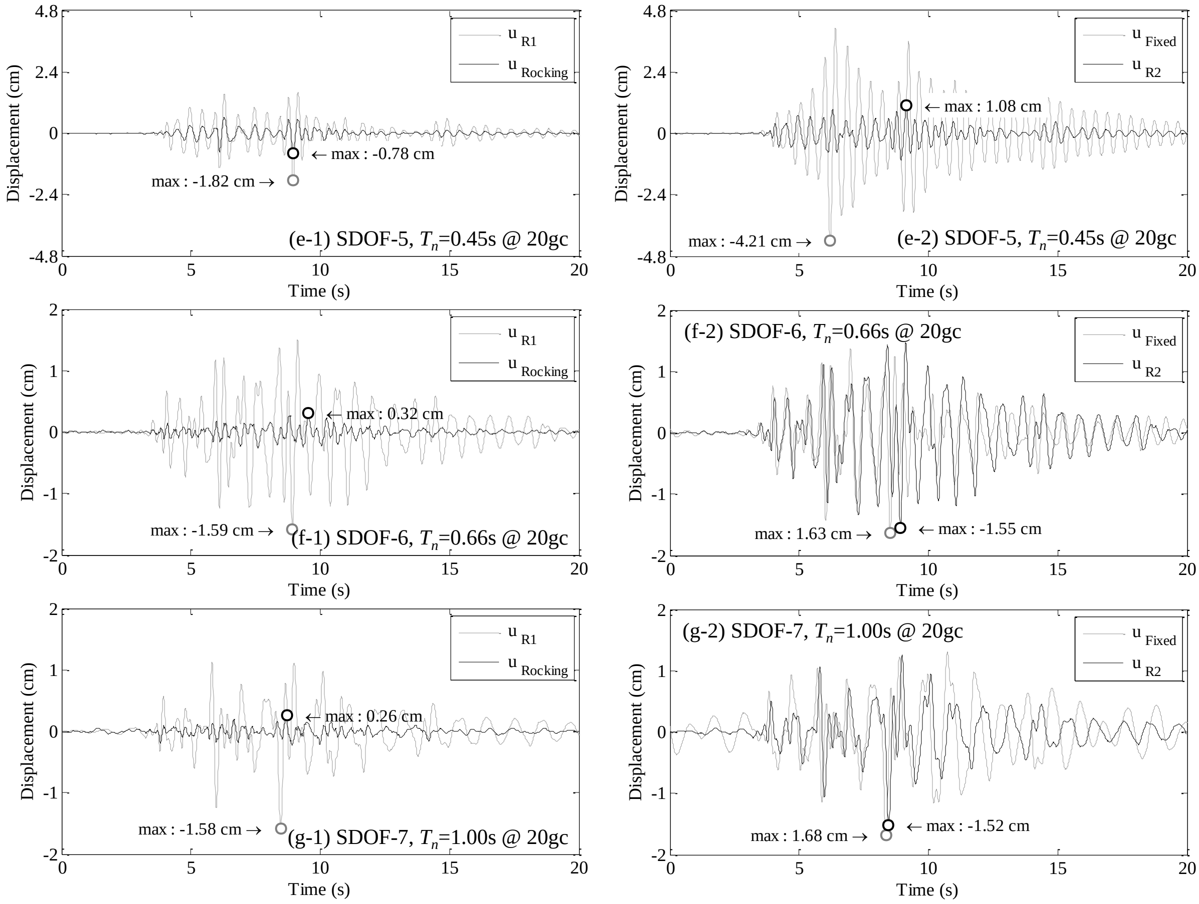

Figure 6. Displacement time history responses of structure models (Northridge, Input PGA=0.22~0.24g) (Cont.)

The lateral force caused by the earthquake motion is expressed by the pseudo-acceleration. In general, the pseudo-acceleration is calculated from the base shear force: $A = V/m$. In this study, the pseudo-acceleration of the prototype structure was calculated from the net lateral displacement u_{R2} as follows.

$$A = \omega_n^2 D \quad \text{where} \quad D = u_{R2} \tag{3.6}$$

At the surface of the soil, an acceleration time history was measured during the earthquake motion. The acceleration at the surface can be regarded as the free field motion of the soil deposit. Usually, the pseudo acceleration of a structure is calculated by applying the free-field motion to the structure model with the fixed base. Figure 7 compares the pseudo-accelerations estimated directly from the measured displacement and the pseudo-accelerations predicted from the free-field motion. Figures 7(a) show the pseudo accelerations of the prototype structures with periods ranging from 0.09s to 0.45s @ 20gc. The predictions from the free-field motion overestimated the measured pseudo accelerations. As mentioned, the rocking effect significantly affected the response of the structures. The rocking displacement induces a radiation damping between the foundation and the sub-soil by increasing the inelastic strain of the soil, which decreases the lateral forces and net displacement of the structure model.

Figure 7(b) show the pseudo accelerations of the structures with periods of 1.33s and 2.00s @ 40g. Since the periods of the structures were different from the site period, the lateral forces were small and the rocking effect decreases. Thus, the correlation of the two pseudo accelerations increased.

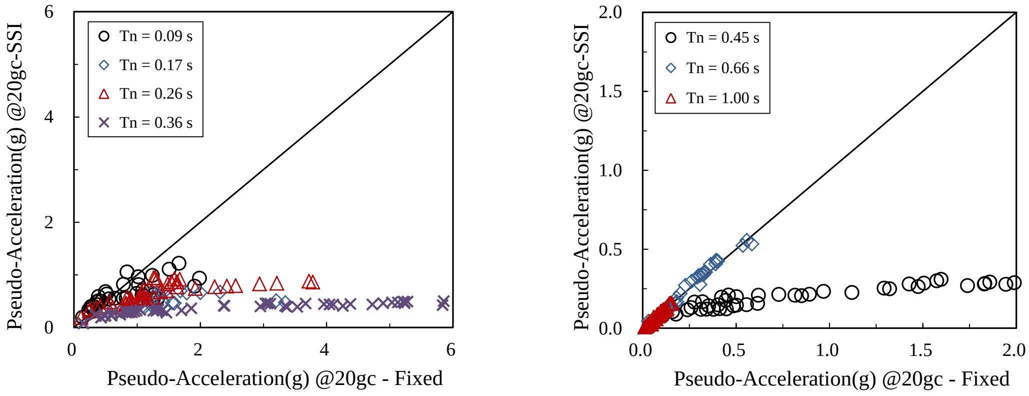

(a) at 20g centrifugal acceleration

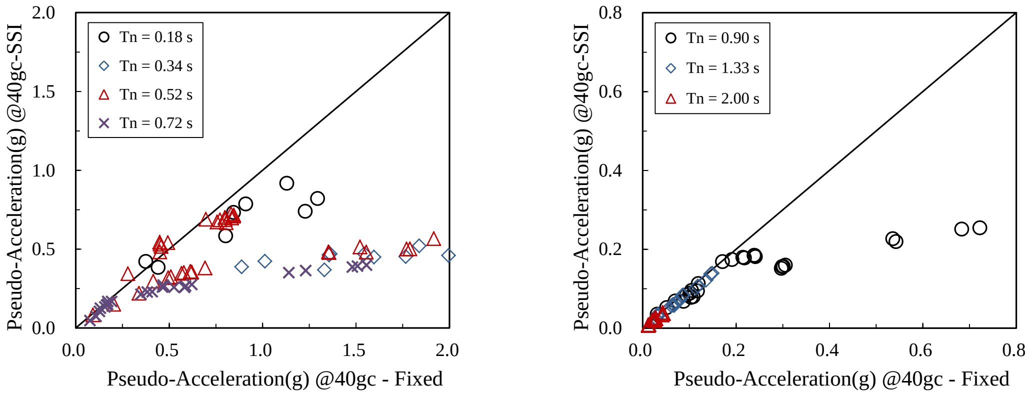

(b) at 40g centrifugal acceleration

Figure 7. Displacements of SDOF structure

4. CONCLUSIONS

The test results reported in this paper show the dynamic response of elastic structures with a shallow mat foundation. When the dynamic periods of the structure models were close to that of the soil deposit, rocking effect became significant, which decreased the net displacement and inertia force of the structure. Thus, unlike expectation, the response of the structure was significantly less than the response predicted by using fixed base and free-field motion. This result indicates that when the response of a structure is increased by the effect of sub-soil, the maximum response is limited by the ultimate moment capacity of the soil and the foundation due to the soil-structure interaction. Thus, in this case, conventional design methods using fixed base and free-field motion may significantly overestimate the response of the structures. However, the safety of the subsoil under the rocking motion should be carefully evaluated.

ACKNOWLEDGEMENT

This work was supported by the National Research Foundation of Korea (NRF) grant funded by the Korea government (the Ministry of Education, Science and Technology) (No. 2010-0027593).

REFERENCES

Chopra A.K. (2007). Dynamics of Structures, Prentice Hall, Upper Saddle River, NJ.

Comartin C.D., Niewiaroski R.W., Freeman S., Turner F.M. (2000). Seismic evaluation and retrofit of concrete buildings: a practical overview of the ATC-40 document. *Earthquake Spectra*. **16(1)**,241-62.

Curras C.J., Boulanger R.W., Kutter B.L., and Wilson D.W. (2001). Dynamic Experiments and Analyses of A Pile-Group-Supported Structure. *Journal of Geotechnical and Geoenvironmental Engineering*.

127(7),585-596.

Das B.M. (2007). Principle of Foundation Engineering, Thomson, Ontario, Canada.

European Committee for Standardization. (2003). EuroCode 8: Design of Structures for earthquake resistance. Brussels.

Gajan S., Kutter B.L., Phalen J.D., Hutchinson T.C., and Martin G.R. (2005). Centrifuge modeling of load-deformation behavior of rocking foundations. *Soil Dynamics and Earthquake Engineering*. **25**,773-783.

Gajan S., Kutter B.L. (2008). Capacity, Settlement, and Energy Dissipation of Shallow Footings Subjected to Rocking. *Journal of Geotechnical and Geoenvironmental Engineering*. **134(8)**,1129-1141.

Gajan S., Kutter B.L. (2009). Contact Interface Model for Shallow Foundations Subjected to Combined Cyclic Loading. *Journal of Geotechnical and Geoenvironmental Engineering*. **135(3)**,407-419.

Hwang H.H.M., Lin H., Huo J. (1997). Site coefficients for design of buildings in eastern United States. *Soil Dynamics and Earthquake Engineering*, **16**,29-40.

International Code Council (ICC). (2009). International Building Code. Country Club Hills, IL.

Kim D.S., Yoon J.K. (2006). Development of New Site Classification System for the Regions of Shallow Bedrock in Korea. *Journal of Earthquake Engineering* **10**,331-358.

Kramer SL. Geotechnical Earthquake Engineering, Prentice hall, Englewood Cliffs, NJ, 1996.

Kutter B.L., Deng L., and Kunnath S. (2010). Estimation of Displacement Demand for Seismic Design of Bridges with Rocking Shallow Foundations. *Proceedings of Fifth International Conference on Recent Advances in Geotechnical Earthquake Engineering and Soil Dynamics*, San Diego, CA.

Mid-America Earthquake Center (MAE center). (1999). Uniform Hazard Ground Motion and Response Spectra for Mid-America Cities, MAE Center Report 03-07, University of Illinois at Urbana-Champaign, IL.

NEHRP. (1997). Commentary on the Guidelines for the Seismic Rehabilitation of Buildings, FEMA publication 274.

Schofield A.N. (1980). Cambridge geotechnical centrifuge operations. *Geotechnique*. **25**,229-267.

Tena-Colunga A., Mena-Hernandez U., Perez-Rocha L. E., Aviles J., Ordaz M., and Vilar J. I. (2009). Updated Seismic Design Guidelines for Model Building Code of Mexico. *Earthquake Spectra*. **25**:869-898.